

Identification of nitric oxide synthase as a protective locus against tuberculosis

(*Mycobacterium tuberculosis*/infectious disease)

JOHN D. MACMICKING^{*||}, ROBERT J. NORTH[†], RON LACOURSE[†], JOHN S. MUDGETT[‡], SHRENIK K. SHAH[§], AND CARL F. NATHAN^{*||}

^{*}Beatrice & Samuel A. Seaver Laboratory, Department of Medicine, Cornell University Medical College, New York, NY 10021; [†]Trudeau Institute, Saranac Lake, NY 12983; and Departments of [‡]Immunology and Inflammation and [§]Medicinal Chemistry, Merck Research Laboratories, Rahway, NJ 07065

Communicated by Maclyn McCarty, The Rockefeller University, New York, NY, March 13, 1997 (received for review December 9, 1996)

ABSTRACT Mutagenesis of the host immune system has helped identify response pathways necessary to combat tuberculosis. Several such pathways may function as activators of a common protective gene: inducible nitric oxide synthase (NOS2). Here we provide direct evidence for this gene controlling primary *Mycobacterium tuberculosis* infection using mice homozygous for a disrupted NOS2 allele. NOS2^{-/-} mice proved highly susceptible, resembling wild-type littermates immunosuppressed by high-dose glucocorticoids, and allowed *Mycobacterium tuberculosis* to replicate faster in the lungs than reported for other gene-deficient hosts. Susceptibility appeared to be independent of the only known naturally inherited antimicrobial locus, *NRAMP1*. Progression of chronic tuberculosis in wild-type mice was accelerated by specifically inhibiting NOS2 via administration of N⁶-(1-iminoethyl)-L-lysine. Together these findings identify NOS2 as a critical host gene for tuberculostasis.

Tuberculosis, the leading cause of death from infectious disease (1), poses an even greater threat as immunodeficiency spreads among the host population and drug resistance rises in the pathogen, *Mycobacterium tuberculosis* (Mtb). A genetic search for mammalian host resistance pathways has revealed increased mycobacterial lethality in mice rendered deficient in T cell subsets [via chromosomal disruption of β_2 -microglobulin, T cell receptor- β , T cell receptor- δ , or recombination-activating gene *RAG2*] (2–4) or in those cytokines and their receptors responsible for macrophage activation [interferon- γ (IFN- γ), IFN- γ receptor, or tumor necrosis factor receptor-1 (TNFR1)] (5–8). Other mice harboring mutations in either the interferon regulatory factor-1 or natural resistance-associated macrophage protein 1 (*NRAMP1*) loci are more permissive for growth of the attenuated bacillus Calmette–Guérin (BCG) vaccine strain of *Mycobacterium bovis* (9, 10).

At least five of the above transgenic lines have been examined for expression of the immunologically induced antimicrobial enzyme, nitric oxide synthase (NOS2) (11); all were found to be deficient. Impaired NOS2 activity arising as a secondary defect suggests that this gene may represent a point of convergence for several mycobacteriostatic pathways. In some studies, the antimycobacterial responses of IFN- γ , TNF- α - or granulocyte-macrophage colony-stimulating factor-treated mouse and human macrophages have been blocked by NOS inhibitors (12–15), and such inhibitors exacerbated the course of disease in mice (16). Moreover, NOS2 was expressed in pulmonary alveolar macrophages from patients with tuberculosis (17). These observations underscore that NOS2 may repre-

sent a pivotal protective locus against tuberculosis, a hypothesis examined here using gene-targeted mice devoid of NOS2.

EXPERIMENTAL PROCEDURES

Mice. Adult (8–12 weeks) male and female NOS2^{-/-} mice (18) and their wild-type or heterozygous littermates were F₂₋₃ (129/SvEv \times C57BL/6) intercross progeny derived from our specific pathogen-free colony maintained at The Rockefeller University, before shipment to the Trudeau Institute. Experiments were performed according to each institutions' guidelines for animal use and care.

Mycobacterial Infection and Enumeration. Mtb (Erdman strain; Trudeau Mycobacterial Culture Collection No. 993) was supplied as frozen (-70°C) log phase dispersed cultures in Proskauer and Beck medium (Difco) containing 0.01% Tween 80 and live bacilli administered via the lateral tail vein as previously described (3). Inoculum dose was corroborated by plating aliquots of the original injectate and 24-hr-infected organ homogenates (10-fold serial dilutions in PBS, 0.01% Tween 80) onto enriched agar (Middlebrook 7H11, Difco) and colony-forming units (CFU) enumerated in triplicate 21–28 days later. Mice were genotyped before experimentation via Southern blot hybridization analysis (18) and verified immediately postmortem by that or PCR.

NOS2 PCR Genotyping. Tail biopsy DNA was prepared as described by Laird *et al.* (19), and 400–600 ng was analyzed by PCR in a 50- μl reaction volume containing 10 mM Tris-HCl (pH 8.3), 50 mM KCl, 1.5 mM MgCl₂, 200 mM dNTPs, and 2.5 units of *Taq* polymerase (Perkin-Elmer). Primer pairs (200 nM each) were as follows: 5' primer (5'-ATCAGCCTT-TCTCTGCTCC-3'), 3' primer (5'-GGCTTTCTGCTGT-TCTCTC-3'), wild-type allele (413-bp amplifcand); 5' primer (5'-GAGCAATGTGACAAAGCTCCTTCAGACTAG-3'), 3' primer (5'-GCCTGAAGAACGAGATCAGCAGCCTC-TG-3'), targeted allele (1,288-bp amplifcand). PCR amplification was performed for 40 cycles, each cycle consisting of 30 s at 94°C, 45 s at 62°C, and 3 min at 72°C before electrophoretically separating the products on a 1.2% agarose gel and visualizing by ethidium bromide staining. A 1:1 correspondence was observed with mice genotyped by Southern blot enlisting a *KpnI-EcoRI* genomic probe (18).

Abbreviations: NOS2, inducible nitric oxide synthase; Mtb, *Mycobacterium tuberculosis*; BCG, bacillus Calmette–Guérin; IFN- γ , interferon- γ ; TNF, tumor necrosis factor; TNFR1, TNF receptor-1; NRAMP1, natural resistance associated macrophage protein 1; CFU, colony-forming unit; RSNO, low molecular weight S-nitrosothiol; p.i., postinfection; AFB, acid-fast bacilli; HC, hydrocortisone; $\beta_2\text{M}$, β_2 -microglobulin; L-NIL, N⁶-(1-iminoethyl)-L-lysine; D-NIL, N⁶-(1-iminoethyl)-D-lysine.

^{||}To whom reprint requests should be addressed. e-mail: cnathan@med.cornell.edu.

[†]Present address: Laboratory of Immunology, The Rockefeller University, New York, NY 10021.

The publication costs of this article were defrayed in part by page charge payment. This article must therefore be hereby marked "advertisement" in accordance with 18 U.S.C. §1734 solely to indicate this fact.

Copyright © 1997 by THE NATIONAL ACADEMY OF SCIENCES OF THE USA
0027-8424/97/945243-6\$2.00/0
PNAS is available online at <http://www.pnas.org>.

NRAMP1 Haplotyping. Identification of *Bcg* polymorphisms at nucleotide 596 was undertaken via the allele-specific PCR method of Medina *et al.* (20). *NOS2*-targeted 129/Sv AB2.1 ES cell (clone 6.16; ref. 18) and C57BL/6 genomic DNAs served as *Bcg^r* and *Bcg^s* standards, respectively.

Plasma NO_x and Low Molecular Weight S-Nitrosothiol (RSNO) Assays. Plasma samples subjected to ultrafiltration (Centricon 10; Amicon) were measured in triplicate for NO₂⁻ + NO₃⁻ by nitrate reductase-linked diazotization assay (18) and RSNOs after Hg²⁺ ion displacement (21). S-Nitroso-L-glutathione (>98% pure; Alexis Chemicals, San Diego) served as the RSNO standard, with linear detection limits of 1.5–200 μM. NO₂⁻ constituted < 4% of total plasma NO_x, and was removed by treatment with 0.5% (wt/vol) H₂NSO₄NH₄ before RSNO determination.

Immunohistochemistry. Ultrathin (2 μm) sections of formalin-fixed, paraffin-embedded lung tissue were incubated overnight at 4°C with rabbit anti-holo MuNOS2 IgG (22) (1:1,000 dilution), and a biotinylated goat anti-rabbit IgG applied before visualizing with avidin-biotin horseradish peroxidase (Vector Laboratories) using 3-amino-9-ethylcarbazole (Sigma) as substrate (23). Sections were counterstained with hematoxylin. Immunoreactive foci were absent in *NOS2*^{-/-} mice, and in *NOS2*^{+/+} mice if either preimmune serum was used or the primary IgG omitted. Substitution of the latter by an anti-MuNOS2 peptide antibody (NO16; ref. 24) (1:500 dilution) gave staining concordant with the anti-holo MuNOS2 IgG.

Histology. Formalin-fixed, paraffin-embedded tissues were sectioned (4–6 μm) and stained with hematoxylin and eosin or by the Ziehl–Neelsen method for acid-fast bacilli (AFB) as described (25).

Cytokine ELISA Analysis. Undiluted plasma samples were assayed in triplicate for MuIFN-γ and MuTNF-α by ELISA (Duo Set; Genzyme). Assay sensitivity ranged between 25 and 810 pg/ml for IFN-γ and 70–2,250 pg/ml for TNF-α.

NOS2 Inhibitors and *in Vivo* Administration. N⁶-(1-Iminoethyl)lysine (NIL; L- and D-enantiomers) were synthesized as the hydrochloride salts (26) and supplied in acidified (pH 2.7) drinking water (4 mM) ad libitum beginning on day 41, and the supply changed every 48 hr through day 70 postinfection (p.i.). Efficacy was assessed by plasma NO_x and RSNO assays before (day 30 p.i.) and during (day 69 p.i.) NIL administration. Neither enantiomer affected food nor water consumption, and necropsy revealed no sign of drug toxicity. Hydrocortisone acetate (United Research Laboratories, Philadelphia) was administered subcutaneously (2.5 mg; 100 mg·kg⁻¹) on days 5 and 10 p.i. for primary Mtb infection (10⁶ CFU) or 40 and 45 p.i. for Mtb reactivation (10⁵ CFU). Nonimmunosuppressed control groups received vehicle (0.2 ml) PBS alone.

Statistical Analysis. Log rank product limit estimates were applied to Kaplan–Meier survival data for determining significance by *F* statistics between two or more groups. Unpaired *t* tests and one-way ANOVA at 95% confidence intervals were performed using InStat PC software, Version 2.00 (GraphPad, San Diego).

RESULTS

NOS2^{-/-} Mice Rapidly Succumb to Mtb Infection. Whether *NOS2* is essential for the orchestrated cellular immune response mounted by the host during primary tuberculosis was evaluated by inoculating *NOS2*^{-/-} mice i.v. with 10⁵ virulent Mtb Erdman bacilli. Consolidating pneumonitis and death were observed within 33–45 days (mean 37.7 ± 1.2 days) p.i. (Fig. 1*a*). Wild-type or heterozygous 129/SvEv × C57BL/6 F₂₋₃ littermates survived a mean 160.0 ± 17.1 days and 151.3 ± 16.5 days, respectively. AFB were abundant within large, sometimes necrotizing, granulomatous lesions in *NOS2*^{-/-}

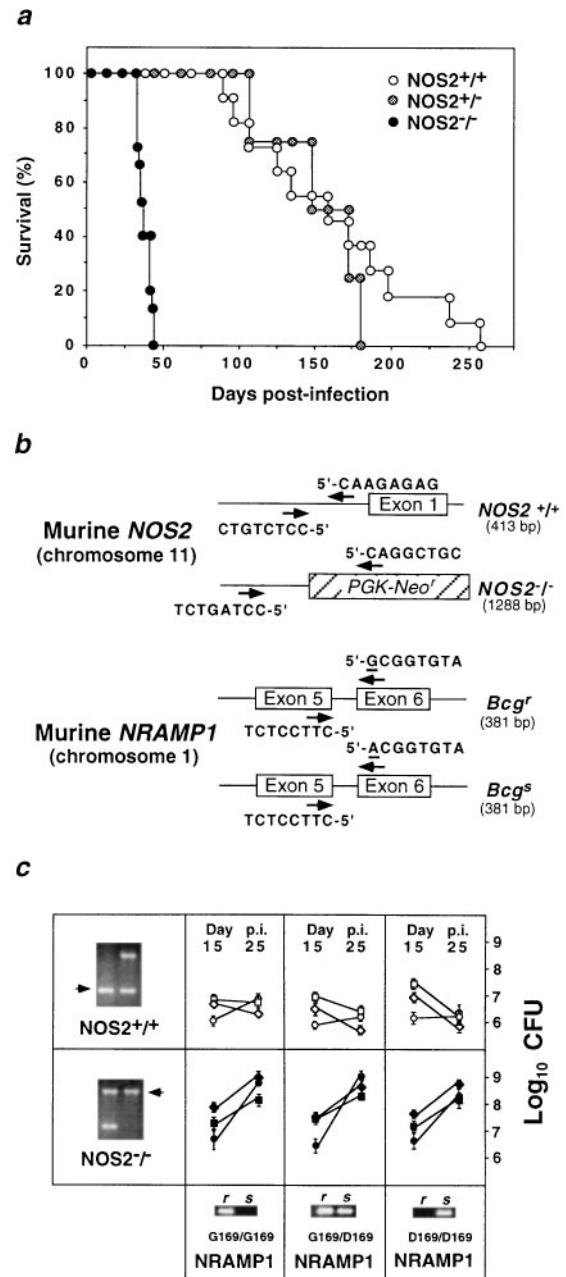


FIG. 1. Absence of *NOS2* confers susceptibility to primary Mtb infection. (a) Survival curves of litter-matched *NOS2*^{-/-} ($n = 15$), wild-type ($n = 11$), and heterozygous mice ($n = 4$) mice injected i.v. with 10⁵ CFU of Mtb Erdman bacilli. Data are from two independent experiments. Differences between *NOS2*^{+/+} or *NOS2*^{+/-} and *NOS2*^{-/-} were statistically significant ($P < 0.0001$, log-rank test). (b) Genotypic and haplotypic allele-specific PCR strategies. Primer positions (arrows) for murine *NOS2* originate within the antisense phosphoglycerate kinase-Neo^r targeted insertion (hatched box) or 5' untranslated region sequences. Terminal 8-bp template sequences are shown. Sizes of the expected amplicands are in brackets. *NRAMP1* primer pairs flank intron 5, with the 3' polymorphic substitution (nucleotide 596) underlined. (c) *NRAMP1* haplotype distribution versus Mtb growth (mean ± SEM) in the lungs (○, ●), livers (□, ■), and spleens (◇, ◆) of *NOS2*^{+/+} (*Bcg^r*, $n = 7$; *Bcg^s*, $n = 3$) and *NOS2*^{-/-} mice (*Bcg^r*, $n = 9$; *Bcg^s*, $n = 5$), respectively. (Inset) PCR amplicands of inherited *NRAMP1* variant alleles (r, *Bcg^r*; s, *Bcg^s*) and intact or targeted *NOS2* alleles (arrows), the latter shown with a *NOS2*^{+/-} control.

lungs, livers, and spleens examined shortly before mice succumbed to infection. In contrast, few AFB were evident in the same organs of control mice at day 30 p.i. (Figs. 1*c* and 2).

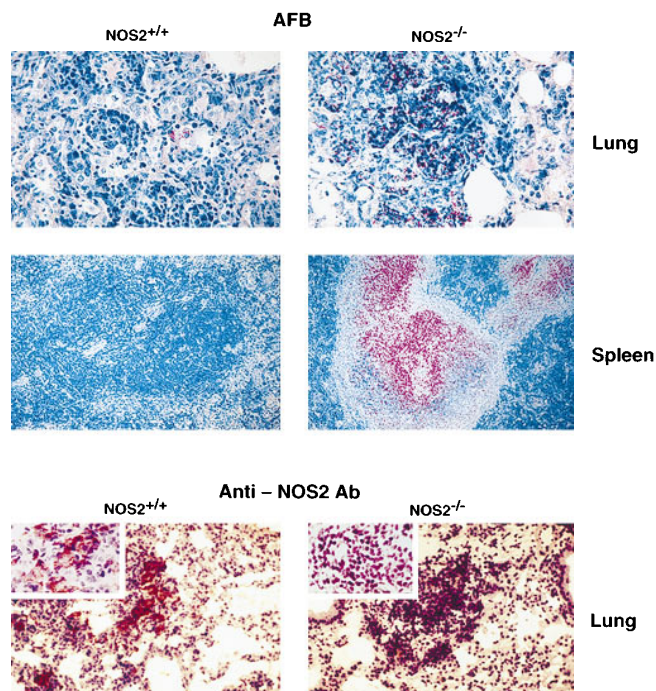


FIG. 2. Presence of AFB correlates inversely with *NOS2* expression in *NOS2*^{+/+} and *NOS2*^{-/-} hosts. Histological analysis of AFB in diseased organs at day 30 p.i. stained by the Ziehl-Neelsen method. Acid-fast bacterial rods appear red. Magnification 400 \times (lung) and 100 \times (spleen). Localized *NOS2* expression in lung granulomas assessed by immunohistochemistry using anti-Mu*NOS2* antibody. Magnification 200 \times . (Inset) 1,000 \times . At least six mice of each group were examined.

Immunohistochemistry revealed the presence of macrophage *NOS2* antigen within lung granulomas of *Mtb*-infected wild-type mice and its absence in *NOS2*^{-/-} mice, although granulomas appeared equally well formed in either genotype (Fig. 2). Plasma $\text{NO}_2^- + \text{NO}_3^-$ confirmed the marked immunologic induction of high-output NO production in wild-type hosts by *Mtb* infection (31.3 ± 4.2 , 177.0 ± 5.1 , and 136.3 ± 10.9 μM at days 1, 15, and 30 p.i.), while failing to increase NO secretion in *NOS2*^{-/-} mice (21.4 ± 2.7 , 26.4 ± 2.0 , and 24.8 ± 2.5 μM at days 1, 15, and 30 p.i.). *S*-nitrosothiols, recently shown to mediate antibacterial effects during murine *Salmonella typhimurium* infection (27), also were elevated in wild-type (6.8 ± 2.1 , 18.3 ± 3.2 , and 14.4 ± 2.4 μM at days 1, 15, and 30 p.i., respectively) versus mutant mice (5.8 ± 1.6 , 6.2 ± 1.2 , and 4.8 ± 1.5 μM at days 1, 15 and 30 p.i.). The lower production of NO by heterozygotes (plasma $\text{NO}_2^- + \text{NO}_3^-$, 63.4–71.5%; RSNO, 54.6–82.4% that of the increase in *NOS2*^{+/+} mice) appeared sufficient to confer extended protection (>150 days).

***NOS2* Controls *Mtb* Growth Independently of *NRAMP1*.** Parental inbred (129/Sv, C57BL/6) and hybrid descendants respond similarly to Erdman infection (2, 6), suggesting the introduced defect, and not strain polymorphisms, account for the susceptibility of *NOS2*^{-/-} offspring. Moreover, by using intercross progeny at F₂ or later generations, any additive effects of the *NRAMP1* (*Bcg*) locus with *NOS2* can be tested, because the 129/Sv and C57BL/6 strains possess resistant (Gly¹⁶⁹) and susceptible (Asp¹⁶⁹) autosomal *Bcg* alleles, respectively (10, 28). Nonconservative replacement of Gly¹⁶⁹ by Asp¹⁶⁹ arises from a recessive point mutation at nucleotide 596; a PCR-based haplotype mapping strategy was enlisted to discriminate between allelic variants and hence the *Bcg*^r and *Bcg*^s phenotype (Fig. 1b). *NRAMP1* segregated independently of resistance to growth of *Mtb* Erdman, as noted for *Mtb* H37Rv (20, 25), and of *NOS2* status (Fig. 1c). Antimicrobial

synergism between these two loci has been speculated (29, 30), but cooperative effects were not apparent in the present experiments. At lower i.v. inocula ($\leq 10^3$), minor resistance to *Mtb* growth ($\leq 0.5 \log_{10}\text{CFU}$) in *Bcg*^r versus *Bcg*^s mice has been reported (31), although not at doses similar to those given here (20, 25). In neither case was *NOS2* status examined.

Monogenic *NOS2* Defect Versus Broad Immunosuppression. Having identified *NOS2* as a monogenic determinant of resistance to *Mtb*, we next evaluated the impact of its absence by comparison with broad immunosuppression. Parenteral glucocorticoid administration has long represented the means by which mice are rendered most vulnerable to tubercular infection (32, 33), even in mice already immunocompromised, such as those with severe combined immunodeficiency (3). Accordingly, *NOS2*^{+/+} and *NOS2*^{-/-} mice were treated with a hydrocortisone (HC) regimen previously shown to suppress mycobacterial resistance both in severe combined immunodeficiency hosts and in uncompromised mice of identical major histocompatibility complex haplotype (H-2^b) to those used here (3). Survival times and mortality rates were similar between vehicle (PBS)-treated *NOS2*^{-/-} mice (mean 28.0 ± 1.0 days, 100% lethality) or HC-injected wild-type (mean 26.7 ± 0.6 days, 100% lethality) and HC-recipient *NOS2*^{-/-} animals (mean 23.3 ± 1.1 days, 100% lethality) after i.v. injection with 10^6 CFU of *Mtb* Erdman (Fig. 3a). In all three groups, bacillary burdens were significantly greater than for vehicle-treated wild-type mice at days 20 and 25 p.i. (Fig. 3b). In the lungs, *Mtb* multiplied $10^{4.95}$ -fold in unsuppressed *NOS2*^{-/-} mice, $10^{5.10}$ -fold in HC-suppressed *NOS2*^{-/-} mice, and $10^{5.09}$ -fold in steroid-treated *NOS2*^{+/+} mice. In healthy controls, bacilli multiplied by a factor of $10^{2.91}$ and plateaued thereafter. A comparable pattern was evident within the liver and spleen, albeit at lower titers (Fig. 3b).

Increases in wild-type plasma $\text{NO}_2^- + \text{NO}_3^-$ and RSNO levels examined 5 days after the last steroid injection were 73.9% and 86.5% lower than that for the PBS-treated group (Fig. 4a). This suppression of inducible NO production persisted through day 20 p.i., coincident with the onset of tubercular signs and death (Fig. 4a). Reduced *NOS2* expression after HC treatment also was observed locally within the lung by immunohistochemistry (data not shown).

***NOS2* Is a Crucial Innate Resistance Gene: Comparison with Other Tuberculostatic Loci.** Clonal expansion of antimycobacterial T cells peaks 3–4 weeks after i.v. *Mtb* Erdman inoculation (34). By such time, the majority of *NOS2*^{-/-} and HC-treated mice either are already ill or have died (Fig. 3a), suggesting that innate resistance is crucial in determining survival outcomes in naive mice. Net *in vivo* doubling times of *Mtb* during days 1–15 thus were used to assess host immunity early after infection (3, 35). Comparison with all reported studies involving i.v. challenge with *Mtb* Erdman in genetically manipulated mice [IFN γ ^{-/-}, TNFR1^{-/-}, or β_2 -microglobulin ($\beta_2\text{M}$)^{-/-}] revealed that replication within the lungs and spleen was fastest in *NOS2*^{-/-} animals, with or without hydrocortisone treatment (Table 1). However, *Mtb* doubling times were comparable for IFN γ ^{-/-}, TNFR1^{-/-}, and *NOS2*^{-/-} mice as a fold-increase over their respectively matched H-2^b-compatible wild-type controls.

Such unilocus similarities may arise because of known *NOS2* deficiencies in IFN γ ^{-/-} and TNFR1^{-/-} mice (5, 6) or, alternatively, because *NOS2*^{-/-} mice might possess immunologic defects involving IFN- γ and TNF- α , which predispose them to tuberculosis. To examine the latter possibility, plasma IFN- γ and TNF- α were measured; both were elevated by day 15 p.i., irrespective of *NOS2* status (Fig. 4b). In fact, IFN- γ levels were 2–3 times higher in *NOS2*^{-/-} mice, perhaps in response to the continued presence of replicating bacilli (Fig. 4b). Detectable IFN- γ and TNF- α declined through day 25 p.i., but still remained above initial (24-hr p.i.) levels (data not shown). HC

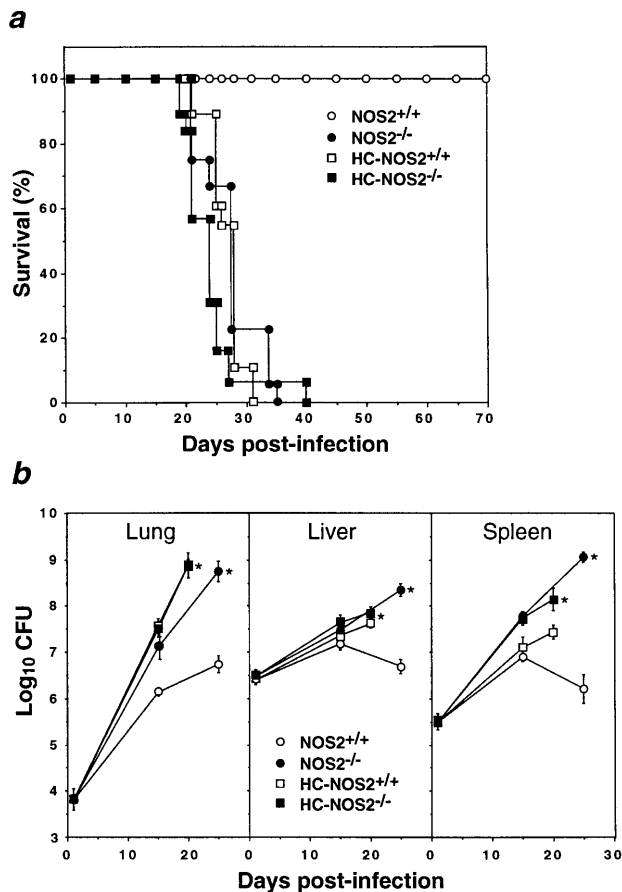


FIG. 3. Phenotypic similarity of NOS2-deficient and glucocorticoid-immunosuppressed mice infected with Mtb. (a) Survival times for Mtb Erdman-infected (10^6 CFU i.v.) mice given 2.5 mg of HC s.c. on days 5 and 10 p.i. NOS2^{+/+} ($n = 16$); NOS2^{-/-} ($n = 18$). Nonimmunosuppressed control groups received vehicle (0.2 ml PBS) alone. NOS2^{+/+} ($n = 17$); NOS2^{-/-} ($n = 19$). Both HC-treated groups and NOS2^{-/-} mice were significantly different from PBS-treated wild-type controls ($P < 0.0002$, log rank). Data represent two independent experiments. (b) Organ mycobacterial burdens (means \pm SEM) of infected mice ($n = 5$ –10 per time point). HC-treated groups were examined earlier (day 20) due to overt illness. *, $P < 0.0002$ versus the PBS-treated wild-type group, ANOVA.

suppressed TNF- α by 55% to 63% in both groups, consistent with its known pharmacologic actions (36).

Vigilance of NOS2 in Preventing Tubercular Progression. The prolonged survival of wild-type mice (Fig. 1a) prompted us to consider whether NOS2 also might be responsible for restricting microbial growth and chronic progression in the late, clinically quiescent phase of the disease. Organ mycobacterial burdens have begun to decline by day 25 p.i. (Fig. 1c), with few AFB detectable by day 30 p.i. (Fig. 2). Beginning on day 41 p.i., clinically stable NOS2^{+/+} mice received either N⁶-(1-iminoethyl)-L-lysine (L-NIL), the most isoform-specific NOS2 inhibitor known to be potent in other models of infectious disease (23, 37), or its inactive enantiomer, N⁶-(1-iminoethyl)-D-lysine (D-NIL). NOS2 can be >90% inhibited when 9 mM L-NIL is imbibed (23); here, limited supply confined the dosage to 4 mM over 30 days. By day 69 p.i. (day 28 of drug treatment), L-NIL afforded 72% suppression of plasma NO₂⁻ + NO₃⁻ and 64% of RSNO compared with D-NIL, and triggered Mtb growth (0.80–2.06 log₁₀ CFU > D-NIL-treated group, Fig. 5b) with death in 50% of cases by the end of treatment (Fig. 5a). As a positive control (38), another group was injected subcutaneously with HC on days 45 and 50 p.i. This also led to disease exacerbation, with 75% mortality by day 70 p.i. (Fig. 5a) associated with large increases in

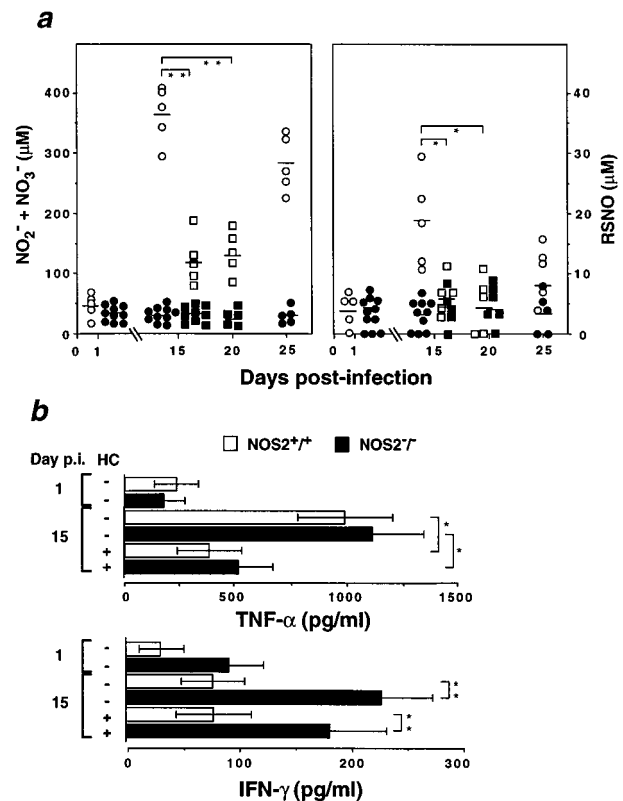


FIG. 4. Suppressive effects of HC on inducible NO production and tuberculostatic cytokines. (a) Release of NO₂⁻ + NO₃⁻ and RSNO during the course of infection and the effects of HC on their secretion. Symbols are as in Fig. 3 and represent individual sera assayed in triplicate; horizontal bars denote group means. *, $P < 0.01$, **, $P < 0.0001$, unpaired *t* test. (b) Plasma TNF- α or IFN- γ responses (mean \pm SEM) of PBS- and HC-treated mice determined in triplicate by ELISA. *, $P < 0.048$, **, $P < 0.038$.

bacillary burden (Fig. 5b). In contrast, D-NIL-treated mice continued to restrict Mtb replication throughout the period of treatment (days 41–70 p.i.; Fig. 5b) and survived for the duration of the experiment (day 90 p.i.; Fig. 5a).

DISCUSSION

These results formally demonstrate that the NOS2 locus is necessary to control primary tuberculosis in mice. Absence of NOS2 led to rapid bacterial growth, necrotic granulomatous pneumonitis, and death. Despite a 30% to 40% reduction in NO release accompanying the loss of one NOS2 allele, heterozygotes still retained sufficient NOS2 activity to extend their survival as long as mice possessing the full chromosomal complement. Additional loci may partially compensate for this loss, although based on the inability of *Bcg*^r inheritance to affect Mtb growth in either NOS2^{-/-} or NOS2^{+/+} mice at the inocula studied here, *NRAMP1* appears an unlikely candidate.

Murine macrophage-derived oxidants such as H₂O₂, O₂⁻ and OH \cdot could represent another avenue of compensation. Singly they appear ineffectual against Mtb Erdman (15); however, evidence is accumulating that both H₂O₂ and O₂⁻ can synergize with NO-derived species to enhance microbial killing (39, 40). Respiratory burst responses in IFN- γ -activated peritoneal macrophages triggered by a mycobacterial agonist were intact in NOS2^{-/-} mice (18). The possibility exists, therefore, that in heterozygous mice these oxidative species may react with the smaller amounts of NO produced to embellish its antitubercular action.

Cooperative antimicrobial effects of NO and another redox partner also may extend to the RSNOs, which increased

Table 1. Comparison of net *in vivo* doubling times for Mtb Erdman in genetically deficient hosts

	Genotype	<i>n</i>	Inoculum	Treatment	Doubling time, hr		
					Lung	Liver	Spleen
(i)*	NOS2 ^{+/+} (B6 × 129 F ₂₋₃)	15	10 ⁶	Vehicle (PBS)	45	130	72
	NOS2 ^{-/-} (B6 × 129 F ₂₋₃)	20	10 ⁶	Vehicle (PBS)	31	92	44
	NOS2 ^{+/+} (B6 × 129 F ₂₋₃)	15	10 ⁶	Hydrocortisone	27	104	63
	NOS2 ^{-/-} (B6 × 129 F ₂₋₃)	20	10 ⁶	Hydrocortisone	27	85	46
(ii)†	IFN-γ ^{+/+} (B6 × 129 F _n)	12	10 ⁶	Untreated	51	319	162
	IFN-γ ^{-/-} (B6 × 129 F _n)	12	10 ⁶	Untreated	43	50	70
(iii)‡	β ₂ M ^{+/+} (B6 F _n backcross)	8	10 ⁶	Untreated	63	125	138
	β ₂ M ^{-/-} (B6 F _n backcross)	8	10 ⁶	Untreated	78	214	183
(iv)§	TNFR1 ^{+/+} (B6 F ₃ backcross)	6	10 ⁵	Untreated	125	R	288
	TNFR1 ^{-/-} (B6 F ₃ backcross)	6	10 ⁵	Untreated	38	181	55

Doubling times calculated from mycobaccillary counts according to ref. 3 during days 1–15 p.i. with the exception of (iv) (days 10–14 p.i.). Genetic background given in parentheses, and *n* equals the total number of mice for both time points. All inocula administered i.v. R denotes resolving (net replication at day 15 p.i. below day 1 p.i.). *Present study, †from ref. 5, ‡from ref. 2, and §from ref. 6.

several-fold in plasma during Mtb Erdman infection. However, only 5% to 8% of detectable NO was bound to low molecular

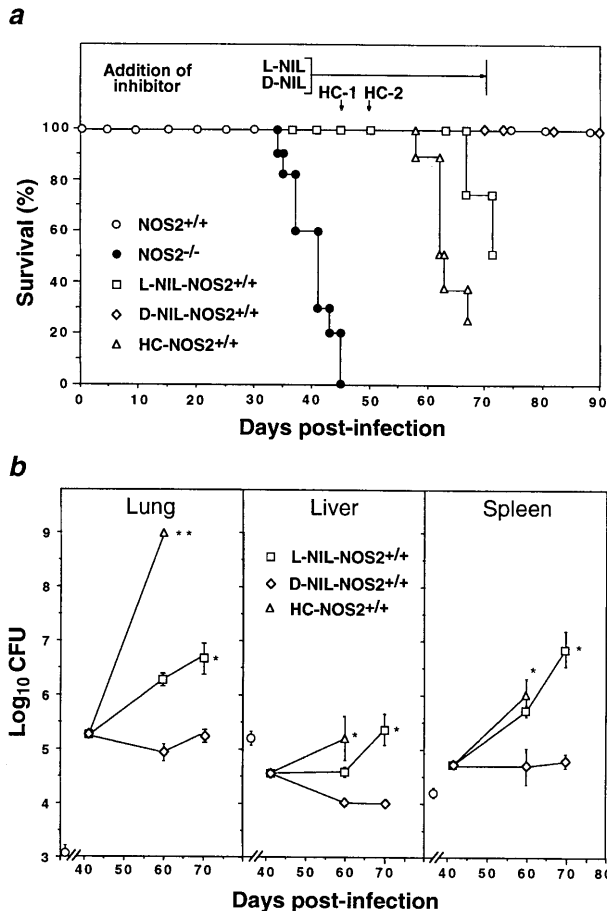


FIG. 5. NOS2 inhibition accelerates disease progression during the clinically quiescent phase of tuberculosis in wild-type mice. (a) Mortality in clinically stable wild-type mice (10⁵ CFU i.v.) receiving 4 mM L-NIL supplied within the period bracketed (*n* = 8) or parenteral HC treatment (2.5 mg) administered s.c. on days 45 (HC-1) and 50 p.i. (HC-2) (*n* = 8). Controls were untreated NOS2^{-/-} (*n* = 10) and NOS2^{+/+} mice (*n* = 10) and NOS2^{+/+} mice given 4 mM D-NIL (*n* = 8). Both L-NIL and HC-treated groups were significantly different from D-NIL-treated wild-type controls (*P* < 0.0005, log rank). (b) Mycobacterial titers (means ± SEM) at the start (day 41 p.i.), within (day 60 p.i.) and at the cessation (day 70 p.i.) of inhibitor treatment (*n* = 4 per time point, with a common pretreatment group). The day 70 p.i. time point was omitted for the HC group due to earlier mortality. Isolated symbols represent recovered inocula on day 1 p.i. *, *P* < 0.01, **, *P* < 0.0001 versus the D-NIL group, ANOVA.

weight thiols, perhaps calling into question their significance in the present studies. Countering this argument is an established history of RSNOs as potent virustatic, parasiticidal, and bactericidal agents (reviewed in ref. 11). Moreover, NO entering the bacterial cell via a thiol adduct (39, 41) may be protected from facile interactions with Mtb outer envelope glycolipids, which can scavenge oxidant species (42). Hence, despite their small quantities, RSNOs nonetheless could have contributed to the antimycobacterial effect.

Regardless of whether NO or one of its derivatives predominated, NOS2 appeared so central for tuberculostatic defense that its disruption had an impact on murine tuberculosis quantitatively equivalent to that of glucocorticoids. Nonsuppressed NOS2^{-/-} mice closely resembled glucocorticoid-suppressed wild types, whereas glucocorticoids had little additive effect in mutant animals. This is consonant with the view that in HC-immunosuppressed wild-type mice, susceptibility may have largely reflected the diminution in macrophage NOS2 expression (43–45). While the lymphoablative effects of glucocorticoids are well documented (reviewed in ref. 36), studies in severe combined immunodeficiency mice demonstrated the existence of residual, glucocorticoid-sensitive resistance to Mtb (3). Whether this non-T cell, non-B cell-dependent resistance pathway involved NK cells cannot be discounted; however, it is more likely to be manifested in macrophages, the cells in which mycobacteria chiefly reside and replicate (3). The experiments described herein provide support for macrophage NOS2 being a major steroid-sensitive tuberculostatic pathway.

TNF-α (55% to 63%) and to a lesser extent IFN-γ (<22%) also were inhibited by glucocorticoids, though neither as much as NO production (74% to 87%). Levels of both cytokines were elevated in the serum of nonsuppressed NOS2^{-/-} mice to the same extent as in wild-type mice, presumably reflecting production at the sites of infection, because the latter represents the stimulus for their release. Indeed, experiments conducted to date have failed to identify immunodeficiencies in NOS2^{-/-} mice other than the introduced defect that could render them susceptible to Mtb infection. Many of the cellular components considered important for the immune response to tuberculosis are unaffected in these mice: CD4 and CD8 single positive T cell populations; TH1 proliferative responses (e.g., to other intracellular pathogens); IFN-γ-up-regulated major histocompatibility complex Class II expression; BCG-triggered respiratory burst responses; and elaboration of IFN-γ and TNF-α, the only cytokines known to activate murine macrophages to inhibit Mtb (18, 46). Of course, other factors not yet examined could be dysregulated.

When germ-line mutations were introduced into several of these protective loci (e.g., IFN-γ, TNFR1, T cell receptor-β, T cell receptor-δ, and β₂M), they, too, allowed virulent Mtb to

establish overwhelming infections (2, 4–6). Of these, IFN- $\gamma^{-/-}$, TNFR1 $^{-/-}$, and $\beta_2M^{-/-}$ mice were examined under comparable conditions (10^5 – 10^6 CFU of Mtb Erdman i.v.) and were of matched or similar genetic background to those NOS2 $^{-/-}$ animals used here. Interstudy comparison of *in vivo* Mtb doubling times thus could be undertaken. Within the lung, these times were shorter in NOS2 $^{-/-}$ mice (27–31 hr) than in the other knock-outs (38–78 hr), approaching the intrinsic replication rate (≈ 20 hr) for Erdman in culture (47). This represents a remarkably permissive environment for Mtb growth and underscores the importance of NOS2 in providing a hostile one. The latter's deficiency in IFN- $\gamma^{-/-}$, IFN- $\gamma R^{-/-}$, and TNFR1 $^{-/-}$ mice implies that NOS2 acts distally to these loci, a suggestion lent further credence by the findings that IFN- γ and TNF- α expression were intact in NOS2 $^{-/-}$ mice, as was granuloma formation.

In mice, as in people, the sterile eradication of Mtb is rarely achieved (33), suggesting that long-term CD4 $^+$ memory T cells must continually enlist the aid of macrophages to maintain bacterial dormancy. A requirement for NOS2 later during infection therefore could be expected if the host is to avoid disease recrudescence. Specifically inhibiting NOS2 with L-NIL during the late phase of clinical stability supported this hypothesis, because infection progressed more quickly and led to earlier mortality. This was observed despite submaximal ($\approx 70\%$) NOS2-specific inhibition. It also may explain why disease acceleration was greater with HC, which, in addition to its suppressive action on mouse macrophage NOS2 expression (44), has direct inhibitory effects on T cell memory (38).

To the extent that findings in mice are germane to man, the fact that NOS2 appears necessary to control mycobacterial growth may have implications for the global incidence of human tuberculosis, because Mtb currently infects over one-third of the world's population (1). A new set of factors thus could influence whether infected individuals develop disease: polymorphisms within the NOS2 locus, the balance of NOS2-inducing or NOS2-inhibiting cytokines (11), clinical use of NOS inhibitors, or the expression of microbial genes that confer resistance to nitroergic products (41, 48).

We thank L. Riley and B. Rogerson for helpful discussions; L. Ryan for histology; and P. Davies and M. McCoss for generous support. This work was supported by National Institutes of Health Grants HL51967 and AI34543 (C.F.N.) and HL51960 (R.J.N.).

1. Raviglione, M. C., Snider, D. E., Jr., & Kochi, A. (1995) *J. Am. Med. Assoc.* **273**, 220–226.
2. Flynn, J. L., Goldstein, M. M., Triebold, K. J., Koller, B., & Bloom, B. R. (1992) *Proc. Natl. Acad. Sci. USA* **89**, 12013–12017.
3. North, R. J. & Izzo, A. A. (1993) *J. Exp. Med.* **177**, 1723–1733.
4. Ladel, C. H., Blum, C., Dreher, A., Reifenberg, K., & Kaufmann, S. H. E. (1995) *Eur. J. Immunol.* **25**, 2877–2881.
5. Flynn, J. L., Chan, J., Triebold, K. J., Dalton, D. K., Stewart, T. A., & Bloom, B. R. (1993) *J. Exp. Med.* **178**, 2249–2254.
6. Flynn, J. L., Goldstein, M. M., Chan, J., Triebold, K. J., Pfeffer, K., Lowenstein, C. J., Schreiber, R., Mak, T. W., & Bloom, B. R. (1995) *Immunity* **2**, 561–572.
7. Dalton, D. K., Pitts-Meek, S., Keshev, S., Figari, I. S., Bradley, A., & Stewart, T. A. (1993) *Science* **259**, 1739–1742.
8. Kamijo, R., Le, J., Shapiro, D., Havell, E. A., Huang, S., Aguet, M., Bosland, M., & Vilcek, J. (1993) *J. Exp. Med.* **178**, 1435–1440.
9. Kamijo, R., Harada, H., Matsuyama, T., Bosland, M., Gerecitano, J., Shapiro, D., Le, J., Koh, S. I., Kimura, T., Green, S. J., Mak, T. W., Taniguchi, T., & Vilcek, J. (1994) *Science* **263**, 1612–1615.
10. Vidal, S., Tremblay, M. L., Govoni, G., Gauthier, S., Sebastiani, G., Malo, D., Skamene, E., Olivier, M., Johty, S., & Gros, P. (1995) *J. Exp. Med.* **182**, 655–666.
11. MacMicking, J., Xie, Q.-W., & Nathan, C. (1997) *Annu. Rev. Immunol.* **15**, 323–350.
12. Denis, M. (1991) *Cell. Immunol.* **132**, 150–157.
13. Denis, M. (1991) *J. Leukocyte Biol.* **49**, 380–387.
14. Flesch I. E. A. & Kaufmann, S. H. E. (1991) *Infect. Immun.* **59**, 3213–3218.
15. Chan, J., Ying, Y., Magliozzo, R. S., & Bloom, B. R. (1992) *J. Exp. Med.* **175**, 1111–1122.
16. Chan, J., Tanaka, K., Carroll, D., Flynn, J., & Bloom, B. R. (1995) *Infect. Immun.* **63**, 736–740.
17. Nicholson, S., Bonecini-Almeida, M. da G., Lapa e Silva, J. R., Nathan, C., Xie, Q.-W., Mumford, R., Weidner, J. R., Calaycay, J., Geng, J., Boechat, N., Linhares, C., Rom, W., & Ho, J. L. (1996) *J. Exp. Med.* **183**, 2293–2302.
18. MacMicking, J. D., Nathan, C., Hom, G., Chartrain, N., Fletcher, D. S., Trumbauer, M., Stevens, K., Xie, Q.-W., Sokol, K., Hutchinson, N., Chen, H., & Mudgett, J. S. (1995) *Cell* **81**, 641–650.
19. Laird, P. W., Zijerveld, A., Linders, K., Rudnicki, M. A., Jaenisch, R., & Berns, A. (1991) *Nucleic Acids Res.* **19**, 4293.
20. Medina, E., Rogerson, B. J., & North, R. J. (1996) *Immunology* **88**, 479–481.
21. Saville, B. (1958) *Analyst* **83**, 670–672.
22. Xie, Q.-W., Cho, H. J., Calaycay, J., Mumford, R. A., Swiderek, K. M., Lee, T. D., Ding, A., Troso, T., & Nathan, C. (1992) *Science* **256**, 225–228.
23. Stenger, S., Donhauser, N., Thurling, H., Rollinghoff, M., & Bogdan, C. (1996) *J. Exp. Med.* **183**, 1501–1514.
24. Xie, Q.-W., Cho, H. J., Kashiwabara, Y., Baum, M., Weidner, J. R., Elliston, K., Mumford, R., & Nathan, C. (1994) *J. Biol. Chem.* **269**, 28500–28505.
25. Medina, E. & North, R. J. (1996) *J. Exp. Med.* **183**, 1045–1051.
26. Moore, W. M., Webber, R. K., Jerome, G. M., Tjoeng, F. S., Misko, T. P., & Currie, M. G. (1994) *J. Med. Chem.* **37**, 3886–3888.
27. De Groote, M. A., Testerman, T., Xu, Y., Stauffer, G., & Fang, F. C. (1996) *Science* **272**, 414–417.
28. Malo, D., Vogen, K., Vidal, S., Hu, J., Cellier, M., Schurr, E., Fuks, A., Bumstead, N., Morgan, K., & Gros, P. (1994) *Genomics* **23**, 51–61.
29. Vidal, S. M., Malo, D., Vogen, K., Skamene, E., & Gros, P. (1993) *Cell* **73**, 469–485.
30. Formica, S., Roach, T. I. A., & Blackwell, J. M. (1994) *Immunology* **82**, 42–50.
31. Brown, D. H., Miles, B. H., & Zwilling, B. S. (1995) *Infect. Immun.* **63**, 2243–2247.
32. Batten, J. C. & McClune, R. M., Jr. (1957) *Br. J. Exp. Path.* **38**, 413–437.
33. McClune, R. M., Jr., Feldmann, F. M., Lambert, H. P., & McDermott, W. (1966) *J. Exp. Med.* **123**, 445–468.
34. Orme, I. M. (1987) *J. Immunol.* **138**, 293–298.
35. Molloy, A., Laochumroonvorapong, P., & Kaplan, G. (1994) *J. Exp. Med.* **180**, 1499–1509.
36. Barnes, P. J. & Adcock, I. (1993) *Trends Pharmacol. Sci.* **14**, 436–441.
37. Stenger, S., Thurling, H., Rollinghoff, M., Manning, P., & Bogdan, C. (1995) *Eur. J. Pharmacol.* **294**, 703–712.
38. Cox, J. H., Knight, B. C., & Ivanyi, J. (1989) *Infect. Immun.* **57**, 1719–1724.
39. De Groote, M. A., Granger, D., Xu, Y., Campbell, G., Prince, R., & Fang, F. C. (1995) *Proc. Natl. Acad. Sci. USA* **92**, 6399–6403.
40. Pacelli, R., Wink, D. A., Cook, J. A., Krishna, M. C., DeGraff, W., Friedman, N., Tsokos, M., Samuni, A., & Mitchell, J. B. (1995) *J. Exp. Med.* **182**, 1469–1479.
41. Hausladen, A., Privalle, C. T., Kneg, T., DeAngelo, J., & Stamler, J. S. (1996) *Cell* **86**, 719–729.
42. Chan, J., Fan, X.-D., Hunter, S. W., Brennan, P. J., & Bloom, B. R. (1991) *Infect. Immun.* **59**, 1755–1761.
43. Rook, G. A. W., Steele, J., Ainsworth, M., & Leveton, C. (1987) *Eur. J. Respir. Dis.* **71**, 286–291.
44. DiRosa, M., Radomski, M., Carnuccio, R., & Moncada, S. (1990) *Biochem. Biophys. Res. Commun.* **172**, 1246–1252.
45. Kunz, D., Walker, G., Eberhart, W., & Pfeilschifter, J. (1995) *Proc. Natl. Acad. Sci. USA* **93**, 255–259.
46. Wei, X.-Q., Charles, I. G., Smith, A., Ure, J., Huang, F.-P., Xu, D., Muller, W., Moncada, S., & Liew, F. Y. (1995) *Nature (London)* **375**, 408–411.
47. Middlebrook, G., Reggiardo, Z., & Tigertt, W. D. (1977) *Am. Rev. Respir. Dis.* **115**, 1066–1069.
48. Nunoshiba, T., De Rojas-Walker, T., Tannenbaum, S. R., & Demple, B. (1995) *Infect. Immun.* **63**, 794–798.